

**Cr(VI) reduction, electricity production, and microbial resistance variation in  
paddy soil under microbial fuel cell operation**

Huan Niu<sup>b</sup>, Can Wang<sup>a\*</sup>, Xia Luo<sup>b</sup>, Peihan Li<sup>b</sup>, Hang Qiu<sup>b</sup>, Liyue Jiang<sup>b</sup>, Subati  
Maimaitiaili<sup>b</sup>, Minghui Wu<sup>b</sup>, Fei Xu<sup>c</sup>, Heng Xu<sup>c</sup>

a State Key Laboratory of Geohazard Prevention and Geoenvironment Protection,  
College of Ecology and Environment, Chengdu University of Technology, Chengdu,  
610059, China

b Sichuan Engineering Research Center for Biomimetic Synthesis of Natural Drugs,  
School of Life Science and Engineering, Southwest Jiaotong University, Chengdu,  
610031, Sichuan, P.R. China

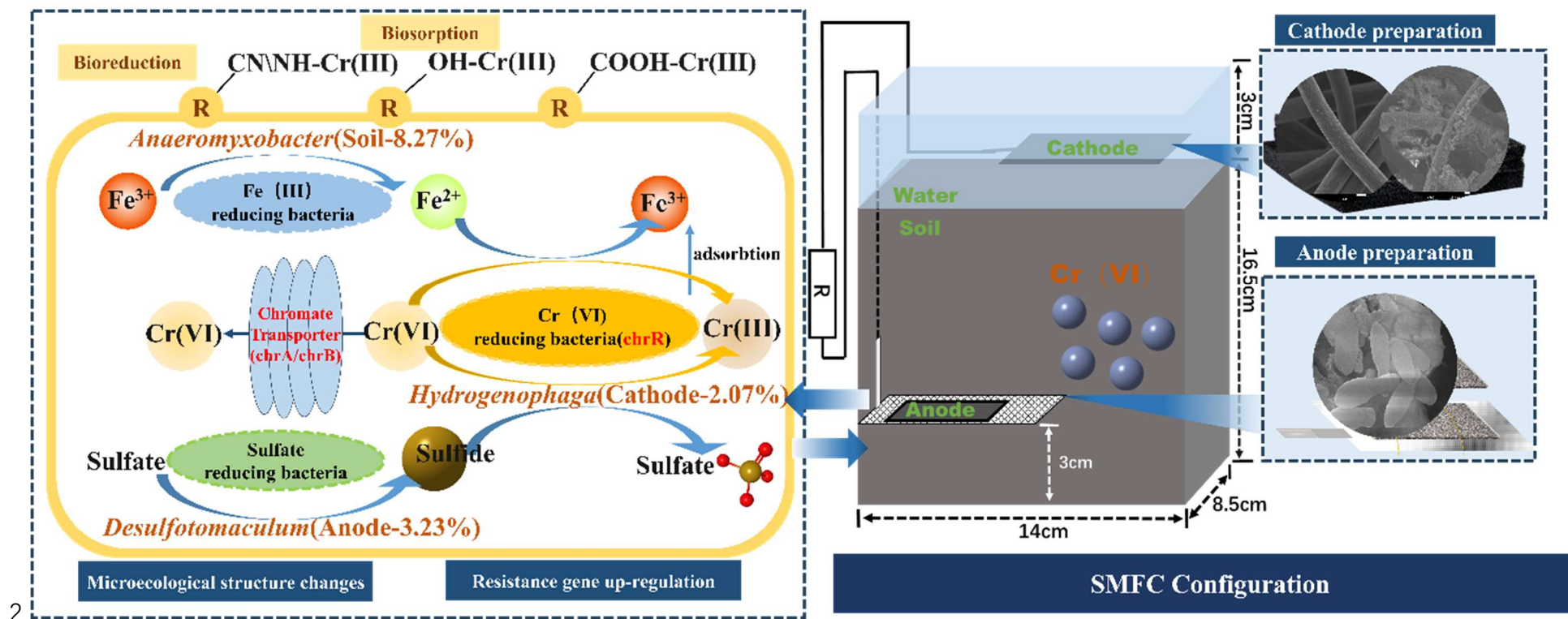
c Key Laboratory of Bio-Resource and Eco-Environment of Ministry of Education,  
College of Life Sciences, Sichuan University, Chengdu 610065, Sichuan, PR China

\* Corresponding at No. 111 Second Ring Road, Chengdu, Sichuan, 610031, China. Tel:  
+ 86 18728156952

E-mail: wangcan@swjtu.edu.cn (Can Wang)

1 Abstract figure:

## "physio-bio" adsorption and reduction of Cr(VI) under bioelectrochemical driving



**Abstract:** Microbial fuel cell (MFC) is an efficient in-situ approach to combat pollutants and generate electricity. This study constructed a soil MFC (SMFC) to reduce Cr(VI) in paddy soil and investigate its influence on microbial community and microbial resistance characteristics. Fe<sub>3</sub>O<sub>4</sub> nanoparticle as the cathodic catalyst effectively boosted power generation (0.97 V, 102.00 mW/m<sup>2</sup>), whose porous structure and reducibility also contributed to Cr reduction and immobilization. After 30 days, 93.67% of Cr(VI) was eliminated. The bioavailable Cr decreased by 97.44% while the residual form increased by 88.89%. SMFC operation greatly changed soil enzymatic activity and microbial structure, with exoelectrogens like *Desulfotomaculum* (3.32% in anode) and Cr(VI)-reducing bacteria like *Hydrogenophaga* (2.07% in cathode) more than 1000 folds of soil. In particular, SMFC operation significantly enhanced heavy metal resistance genes (HRGs) abundance. Among them, *chrA*, *chrB*, and *chrR* increased by 99.54~3314.34% in SMFC anode, probably attributed to the enrichment of potential tolerators like *Acinetobacter*, *Limnohabitans*, and *Desulfotomaculum*. These key taxa were positively correlated with HRGs but negatively correlated with pH, EC, and Cr(VI), which could have driven Cr(VI) reduction. This study provided novel evidence for bioelectrochemical system application in contaminated paddy soil, which could be a potential approach for environmental remediation and detoxification.

**Keywords:** Chromium; Microbial fuel cell; Microbial response; Metal resistance

## Nomenclature

SMFC	Soil microbial fuel cell
HRGs	Heavy metal resistance genes
HMs	Heavy metals
HGT	Horizontal gene transfer
EAB	Electrochemical active bacteria
GF	Graphite felt
ORR	Oxygen reduction reaction
WCV	Working circuit voltage
OCV	Open circuit voltage
ARGs	Antibiotic resistance genes
CMFC-A	Anode of the closed circuit group
OMFC-A	Anode of the open circuit group
CMFC-C	Cathode of the closed circuit group
OMFC-C	Cathode of the open circuit group
CMFC-S	Soil of the closed circuit group
OMFC-S	Soil of the open circuit group
NMFC-S	Soil of the non-electrode control group

## 1. Introduction

Chromium (Cr) is a main toxic heavy metal (HM), that enters the environment mainly due to its wide use in electroplating, tanning, and other industries (Coetzee et al., 2020). Mineral-sourced phosphate fertilizer also contains high-level Cr, promoting its spreading, migration and accumulation in soil and underground water (Chen et al., 2022a). The persistence and toxicity of HMs create permanent and selective stress on environmental microbes. Under the toxic stress, microorganisms have deployed various strategies, including active efflux of the toxic from the microbial cell, regulation of targets, and enzymatic modification of the toxic, presenting as elevation of heavy metal resistance gene (HRG) and tolerant microbe (Van Hoek et al., 2011). Even a sub-dose of Cr (especially the Cr(VI) state) can promote plasmid-mediated horizontal gene transfer (HGT) (Zhang et al., 2018), causing HRG enrichment, threatening environmental safety (Guo et al., 2021; Wang et al., 2020a; Wang et al., 2023b). Meanwhile, due to the co-selection effect, the long-term existence of HMs also causes the enrichment of antibiotic-

resistant bacteria (ARB), further increasing the resistance gene spreading risk in the environment (Men et al., 2018). Such a threat could be more fierce under the coexistence of HMs and antibiotics (Ashbolt Nicholas et al., 2013). Hence, the enrichment of HRGs and ARB under Cr exposure has become an emerging concern.

Common remediation methods for Cr-influenced soil include chemical reduction and leaching (Cong et al., 2022), electrokinetic remediation (Morales-Benítez et al., 2023), and phytoaccumulation (Yaashikaa et al., 2022), which convert Cr(VI) into insoluble and low toxic forms (e.g., Cr(III)) by adsorption, ion exchange, and redox (Rani et al., 2022). Among them, the microbial approach using functional microbes is commonly used for the continuous treatment of soil-groundwater, which has a low cost without side effects (Fan et al., 2023). For example, *Comamonas testosteroni* bacterial strains are used to degrade hexachlorobenzene and *Acinetobacter calcoaceticus* GSN3 strain to degrade phenol (Dimova et al., 2022; Irankhah et al., 2019). However, pollutants can be tightly adsorbed by soil particles and persistently remain (Wang et al., 2023c). The complex soil constituents and competition of indigenous microorganisms inhibit the colonization and development of functional microbes and limit their effectiveness (Guo et al., 2021).

Microbial fuel cell (MFC) technology can transform or immobilize HMs and generate electricity utilizing electrochemical active bacteria (EABs) (Gupta et al., 2023; Chen et al., 2022b), which have been used in sediment or soil to treat HMs and organics and monitor environmental toxicity (Li et al., 2023b). For example, soil microbial fuel cells can mitigate the accumulation of heavy metals in rice and promote the removal of atrazine in the soil (Gustave et al., 2020; Farkas et al., 2024). At present, soil MFC (SMFC) has been used for pollution control, focusing on pollutant content and forms as well as the

electrochemical properties (Hamdan and Salam, 2023; Liu et al., 2023a). There is a lack of systematic research about the MFC effect on soil microbial community structure shifting and resistance characteristics, especially under the HMs contamination circumstance.

In this study, an SMFC was constructed to remediate Cr(VI) contaminated paddy soil. EABs were pre-loaded on the SMFC anode to promote electricity production and Cr transformation. Ferroferric oxide ( $\text{Fe}_3\text{O}_4$ ) nanoparticles, which can reduce and fix Cr(VI) directly, were used as a catalyst for cathodic oxygen reduction reaction (ORR) to improve SMFC performance due to its catalytic effect, non-toxicity, cost-effectiveness, and free of secondary pollution (Liu et al., 2023b). During operation, Cr(VI) was simultaneously reduced and immobilized by bio-physical adsorption and electrochemical-microbial reduction. The Cr(VI) reduction mechanism and the analysis of microbial community structure shaping and HRG variation were comprehensively studied. For the first time, SMFC-driven Cr(VI) reduction was associated with microbial resistance, which evolved along with microbial adaptation and development. This study not only provides a reference for the microbial remediation of polluted soil but also improves the practical field application of MFC. The method can be used for in-situ contaminant treatment in various environments, such as aquaculture ponds, inland lakes, and wetlands.

## **2. Materials and Methods**

### **2.1. Chemicals**

All the chemicals and reagents were analytical grade or premium pure from Kelong Chemical Reagent Factory, Chengdu, China.

## 2.2 Construction of SMFC

### 2.2.1 Soil

Paddy soil from Jintang County, Chengdu, China (30°74' N, 104°59' W) was collected and used to construct SMFC. The soil has organic matter, organic carbon, and total nitrogen of  $8.84\pm0.02\%$ ,  $1.74\pm0.01\%$ , and  $321.67\pm1.25$  mg/kg, respectively. Referring to the previous studies and the Chinese Soil Environmental Quality Standard (GB15618-2018), 120.00 mg/kg potassium dichromate was added to the soil and a final Cr(VI) concentration of 118.80 mg/kg was achieved before use (Liu et al., 2020; Mandal et al., 2017; Li et al., 2024).

### 2.2.2 Electrodes Preparation

Aluminum foam ( $66.00 \times 54.00 \times 5.00$  mm, porosity 60.00-80.00%, bulk density 0.50-1.10 g/cm<sup>3</sup>) (SANZHENG Metal material, Chengdu, China) was used as anode. The anode microflora was derived from municipal sludge (Chengdu Sixth Sewage Treatment Plant, China) after acclimating with 100.00 mg/L Cr(VI). Before assembling, the aluminum foam was cultivated in the anode microflora for 2 weeks. Then the anode was tied to titanium mesh tightly with titanium wire. Graphite felt (GF) ( $100.00 \times 50.00 \times 3.00$  mm, bulk density 0.10-0.15 g/cm<sup>3</sup>) was used as the cathode (Table S1). Before use, it was cleaned, dried, and loaded with Fe<sub>3</sub>O<sub>4</sub> as the ORR catalyst, as detailed in section 1 of the supplementary material. For characterization, we utilized a scanning electron microscope (SEM) to examine the structure and morphology of the electrode surface. In addition, we performed X-ray photoelectron spectroscopy (XPS) and energy dispersive spectroscopy (EDS) to analyze the valence state and element composition. The phase composition was determined using an X-ray diffractometer (XRD).

### 2.2.3 SMFC construction

A plastic box (140.00×85.00×165.00 mm) was used as the SMFC reactor, with 1.50 kg air-dried soil and overlying water of 3.00 cm to simulate the flooded state during rice planting. The cathode was floated on the water surface while the anode was buried (about 3.00 cm from the bottom). The cathode and anode were connected to a 2000  $\Omega$  resistor using titanium wire. The water level was kept constant by daily replenishment (Fig. S1).

## 2.3 Design and Operation

Three treatments were set up as shown in Fig. S1, and three parallels were set for each group. NMFC: The control group with no electrode, only contains an equal amount of overlying water and paddy soil. OMFC: The open circuit group with disconnected electrodes and equal amounts of overlying water and paddy soil. CMFC: The complete closed-circuit SMFC capable of producing electricity, with electrodes connected by a 2000  $\Omega$  resistor, and equal amounts of overlying water and paddy soil.

The experiments were conducted at 25°C. A Raspberry Pi data acquisition system (ARMv7 architecture) was connected at both ends of the resistor of CMFC to monitor the voltage. A multimeter was used for verification. The detailed code information can be found in section 2 of the supplementary material.

Soil and water samples were taken every 5 days until day 35, and the operation continued for another 10 days until day 45 (Specific sampling details are given in the supplementary file). The electrochemical properties of the SMFC including the polarization curve and power density curve were tested using an electrochemical workstation on days 15 and 30 (Ch660e, Shanghai Chenhua Instrument Co., Ltd., Shanghai, China) (Chen et al., 2022b).



## **2.4 Cr Migration and Transformation**

To determine total Cr, 0.50 g soil was subjected to acid digestion (HCl-HNO<sub>3</sub>-HClO<sub>4</sub>) before measurement using flame atomic absorption spectrometry (FAAS) (PinAAcle 900T AA Spectrometer, PerkinElmer, America). To determine Cr speciation, BCR sequential extraction was applied to divide Cr into HOAc extractable, reducible, oxidizable, and residual fractions with mobility and availability from high to low (Wang et al., 2020a). Also, Cr(VI) concentration in overlying water was determined by a spectrophotometer at 540 nm, while Cr(VI) in soil was determined using FAAS after alkaline digestion (Fan et al., 2021). Duplicates, method blanks, and standard reference materials were used for quality control. Cr recovery in standard reference materials was 92.00~108.00%.

## **2.5 Microbial response during operation**

### **2.5.1 Soil biochemical response**

Soil dehydrogenase (DHA) activity was measured using 2, 3, 5-triphenyl tetrazolium chloride (TTC) method. Urease activity was determined by the phenol sodium hypochlorite colorimetric assay. Invertase activity was determined by the 3, 5-dinitro salicylic acid colorimetric assay. The acid phosphatase (ACP) activity was determined by the p-nitrophenyl disodium phosphate colorimetric assay (Wang et al., 2019; Wang et al., 2017).

### **2.5.2 Microbial community structure**

The microbial community structure of the electrodes and soil was determined by high-throughput sequencing (Faust and Raes, 2012; Deng et al., 2012; Bokulich et al., 2018). Majorbio (Shanghai, China) performed 16S rRNA gene sequencing using the Illumina HiSeq platform. 0.50 g of fresh homogenized samples were used to extract the total bacterial DNA with a universal DNA Kit (Omega Biotek Inc.,

USA). After amplification and purification, the V3-V4 hypervariable regions of the bacterial 16S rRNA gene were amplified with primer pairs 338F and 806R. After sequencing, the operational taxonomic units (OTUs) with a 97.00% similarity cut off were clustered using UPARSE version 7.1, and chimeric sequences were identified and removed. The taxonomy of each OTU representative sequence was analyzed by RDP Classifier version 2.2 against the 16S rRNA database using a confidence threshold of 0.7. The alpha diversity, beta diversity, microbial community structure change, and environmental factor correlation analysis were conducted. (Wang et al., 2023a)

### 2.5.3 HRG Fluctuation

Microbial DNA Rapid extraction kit (Shenggong Bioengineering Co., LTD., Shanghai, China) was used to extract total DNA from fresh samples (The extraction method is shown in the supplementary material). The abundance of HRGs in the surface soil of SMFC and OMFC anode after operation was analyzed using an SYBR Green real-time fluorescence quantitative PCR system (7500, Thermo Fisher, USA) (Wang et al., 2023c). The soil of OMFC was used for comparison. The detected genes included HRGs (*chrA*, *chrB*, *chrR*, *recG*, *nfsA*, *zupT*, *fpvA*) and MGEs (*intI*, *tnpA02*, *tnpA04*, *tnpA05*). The primer sequences are provided in Table S2. The specific detection steps were as follows: pre-denaturation at 95°C for 30 s, denaturation at 95°C for 5 s, and annealing and extension at 60°C for 30 s. Forty cycles were performed to make three replicates, and 16S rRNA was used as the internal reference gene. The relative gene expression results were analyzed using the  $2^{(-\Delta\Delta Ct)}$  method, which is commonly used for relative quantification, where  $\Delta\Delta Ct = (Ct \text{ target gene} - Ct \text{ internal reference gene}) \text{ experimental group} - (Ct \text{ target gene} - Ct \text{ internal reference gene}) \text{ control group}$ .

## 2.6 Data analysis

The experimental data were evaluated using one-way analysis of variance (ANOVA) based on three tests. The mean values and standard deviations were calculated using SPSS 22.0 software (IBM, USA). A significance level of  $P < 0.05$  was considered statistically significant, while  $P < 0.01$  was defined as highly statistically significant. Graphs were plotted using Origin 2022 software.

## 3. Results

### 3.1 Electrodes characterization

As demonstrated in Fig. S2, Fig. 1, and Fig. 2, the raw GF had smooth surfaces with C, and O as the main elements (Fig. S2). After  $\text{Fe}_3\text{O}_4$  loading, black patches constituted with spherical particles appeared, bringing Fe (13.17%) and O (19.97%) on the GF surface (Fig. 1a-c and Table S3). XPS revealed that peaks of the cathode GF loaded with catalyst at 710.80 and 724.40 eV were consistent with typical  $\text{Fe}_3\text{O}_4$  peaks (Fig. 2a-b), indicating its successful loading. The CV curves of the cathode (Fig. 2c) presented an obvious oxidation peak at 0.85 V, indicating its excellent electrochemical performance.

Chromium exists mainly in the III and VI oxidation states in soil. The peaks at 576.90 eV and 579.00 eV are typical peaks of Cr(III) and Cr(VI), respectively. After operation, the typical peaks of Cr(III) and Cr(VI) can be observed on the X-ray energy spectra of both cathode and anode, and Cr(VI) and Cr(III) are present on the cathode and anode of SMFC (Fig. 2d-e). The results showed that at least the valence state of Cr changed on the electrode and Cr(VI) was reduced and fixed by the electrode (Kim et al., 2017). GF was found loaded with many soil elements including Cr, Na, Mg, and Ca (Table S3). SEM also observed many microorganism cells and extracellular organic-like substances, implying the biofilm formation on the cathode (Fig. 1d-f).

As presented in Fig. S2C, the raw aluminum foam showed a rough porous structure with mainly Al and O on the surface (Table S3). After loading EAB, many spherical and rod-shaped bacteria were observed, indicating that aluminum foam has a good capacity to carry microorganisms (Fig. 1g-i). After the operation, many millimeter-scale soil particles were embedded in the anode interspace, indicating the intense mass transfer between the anode and soil (Fig. 1j-l).

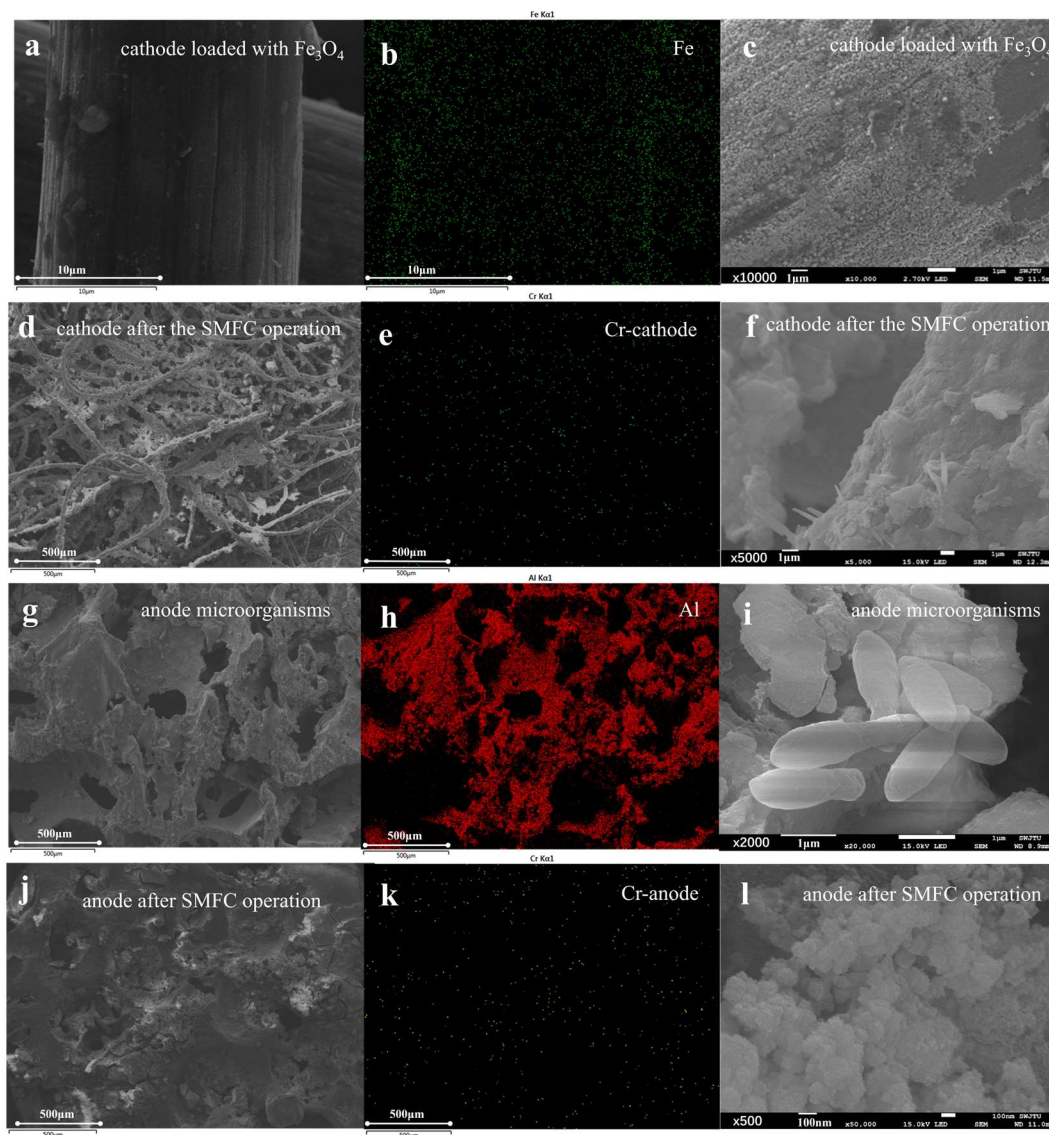
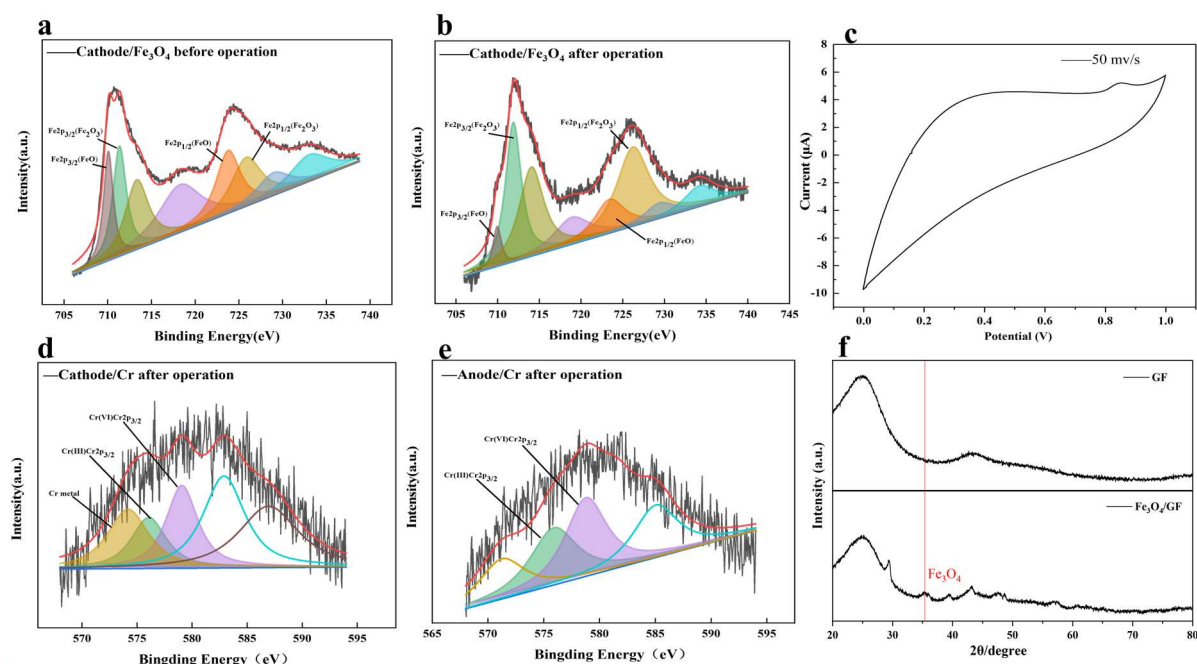
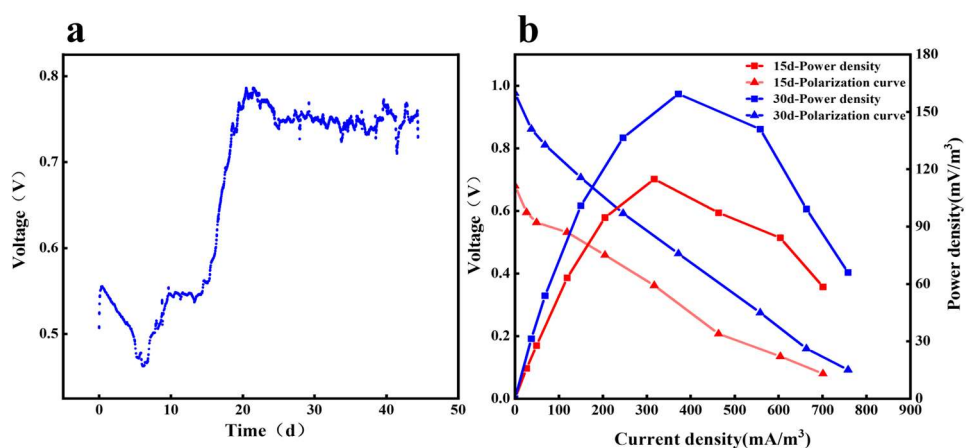


**Fig. 1** Characterization of electrode materials before and after operation by SEM and EDS. (a-c) SEM and EDS images of cathode loaded with  $\text{Fe}_3\text{O}_4$ ; (d-f) SEM and EDS images of cathode after the SMFC operation; (g-i) SEM and EDS images of anode microorganisms; (j-l) SEM and EDS images of the anode

184 after SMFC operation. (Note: The first column is the SEM image, the second column is the corresponding  
 185 EDS, and the third column is the corresponding enlarged SEM image.)



186  
 187 **Fig. 2** Characterization of electrode materials. (a-b) Fe2p spectra of cathode/Fe<sub>3</sub>O<sub>4</sub> composite cathode,  
 188 (c) cyclic voltammetry (CV) curve of cathode/Fe<sub>3</sub>O<sub>4</sub>, (d-e) Cr2p spectra of GF composite cathode and  
 189 Anodic Aluminum foam after operation, (f) XRD spectrum of the cathode-Fe<sub>3</sub>O<sub>4</sub>.



190  
 191 **Fig. 3** Power generation performance of SMFC. (a) SMFC output voltage distribution, (b) 15-day vs. 30-  
 192 day polarization curves and power density curves of the SMFC.

### 3.2 Electricity Generation Performance

Initially, CMFC showed a working circuit voltage (WCV) of 0.55 V and an open circuit voltage (OCV) of 0.68 V (Fig. 3a). In the first week, WCV dropped quickly to 0.45 V but bounced back and stabilized at 0.75 V on day 25, implying the adaption process of the anode microbes in the soil. We reasonably concluded that in the complex heterogeneous environment of soil, the anodic EAB needs some time to adapt to fluctuating environmental conditions facing environmental disturbances. During SMFC operation, the anode microbial community could be gradually selected and enriched, and a stable adaptive community is formed, so the SMFC voltage tends to be stable. This conjecture is also reflected in subsequent results.

On day 15 (OCV of 0.67 V) and day 30 (OCV of 0.97 V), a series of resistors (50~10 000  $\Omega$ ) was connected to the electrodes to determine the polarization curves and power density of the SMFC. As shown in Fig. 3b, the power density increased and decreased with the elevation of external resistance. At 510  $\Omega$ , the power density reached a maximum of 114.90 mW/m<sup>3</sup> (73.50 mW/m<sup>2</sup>) on day 15 and 159.40 mW/m<sup>3</sup> (102.00 mW/m<sup>2</sup>) on day 30 (Table S4). The result indicated that the electrochemical performance of SMFC enhanced gradually probably due to the microbial adaption. Even after 45 days, the CMFC still had a WCV of around 0.75 V, indicating its substantial and stable electricity-producing capacity. Compared with the literature, the SMFC in the current work has an outstanding power generation capacity (Table S5).

### 3.3 Cr(VI) reduction and immobilization during operation

The forms and speciations of HMs determine their bioavailability and toxicity (Jia et al., 2022). After operation, Cr forms in soils were significantly changed ( $P<0.05$ ) (Fig. 4). In CMFC, the acid-soluble Cr

decreased substantially by 97.44%, the oxidizable and reducible fractions did not change significantly, while the residual form of Cr increased by 88.89% (Fig. 4a). However, in NMFC, the acid-soluble Cr increased substantially by 61.54% on day 35. In OMFC, the acid-soluble Cr increased before decreasing, which was opposite to its oxidizable state. On day 35, the Cr bioavailability of OMFC (11.90%) and NMFC (18.90%) was 3866-6200 folds of CMFC (0.30%). It is inferred that the electric field and the microbial communities' evolvement may lead to better Cr immobilization and transform Cr into less toxic forms.

In the meantime, the Cr(VI) concentration (Fig. 4c) dropped in all the groups, and Cr (VI) in CMFC soil was significantly lower than OMFC and NMFC ( $P<0.05$ ) after the experiment. On day 35, CMFC showed 13.59% and 20.87% higher Cr(VI) elimination than OMFC and NMFC, respectively. The overlying water was initially free of Cr. During the experiment (Fig. S3), 0.21~12.72 mg/L Cr was determined, which could be released from the soil. A low level of Cr(VI) (less than 3.15 mg/L) was detected but vanished later (day 15), which could be attributed to the dynamic adsorption-desorption of soil particles and electrodes.

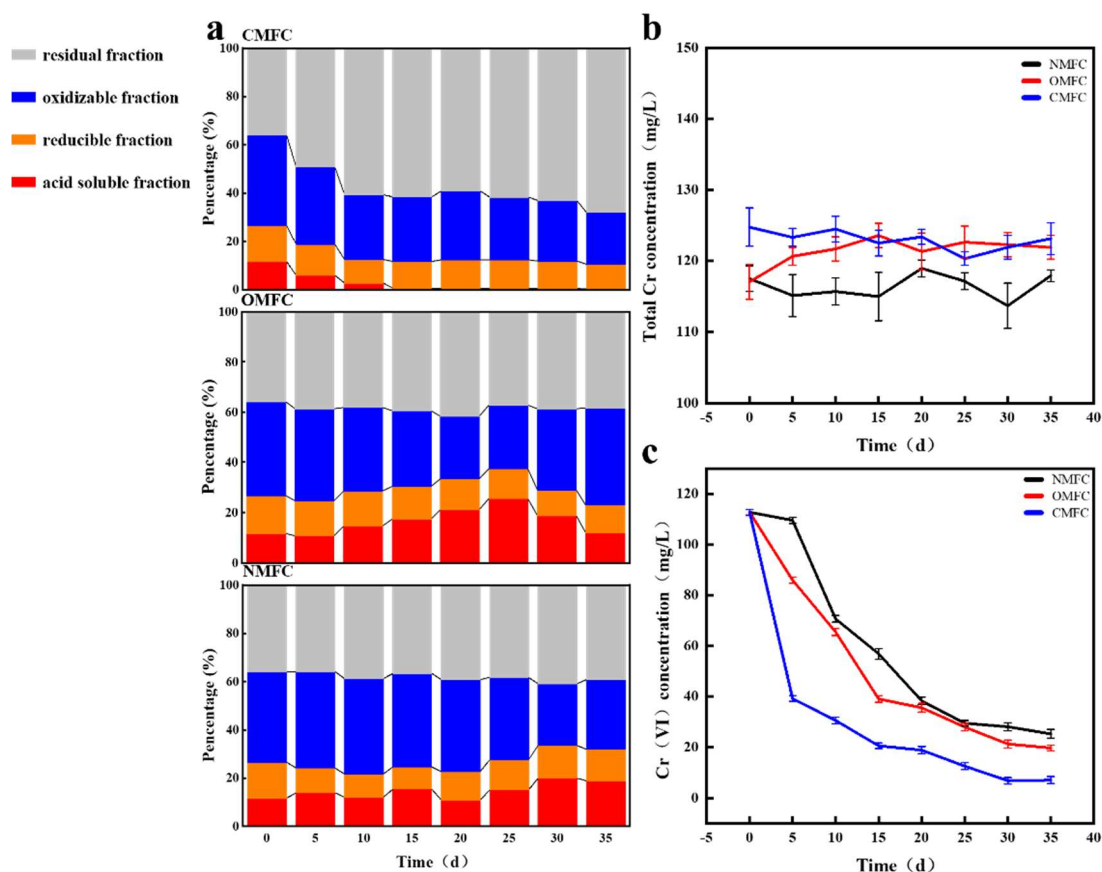


**Fig. 4** Cr speciation and transformation during SMFC operation. (a) Percentage share of Cr in different chemical fractions in CMFC, OMFC, and NMFC soil; Changes in soil (b) total chromium and (c) Cr(VI) concentrations during SMFC operation.

### 3.4 Soil properties

#### 3.4.1 Soil Physicochemical Property

The soil pH decreased in all the groups (Fig. S4A). The soil pH of CMFC decreased fastest from the initial 7.71 to about 6.83 on day 35, with a minimum of 6.77 on day 30, which was 0.14-7.87% lower than others ( $P < 0.05$ ). During the experiment, oxygen in the flooded soil decreased rapidly due to microbial consumption, and acidic products (e.g., low-molecule organic acids) were produced to increase soil acidity. Microorganisms (especially EABs) decompose soil organic matter and release a large number of electrons and protons, making oxidizing substances such as nitrate and high valence metals



(Fe(III), Mn(IV), and Cr(VI)) to accept electrons for reduction, causing protons ( $H^+$ ) accumulation (He et al., 2016). Such a phenomenon was more intense in CMFC due to the rapid electron transfer through wire to the cathode, leaving protons elevated near the anode.

In all the groups, EC increased rapidly from the initial 1.55 ms/cm before stabilizing (Fig. S4B), which maximized 2.60, 2.40, and 2.40 ms/cm in CMFC, OMFC, and NMFC ( $P>0.05$ ), respectively. The rapid increase in EC could be attributed to the inundation that increased the soluble salt content of the soils. The electromigration in the MFC electric field may also increase soil mass transfer and positively affect soil electrical conductivity (Zhang et al., 2020).

#### 3.4.2 Soil Biochemical Response

Soil enzyme activity is an important index to evaluate soil environmental change. Soil enzymes, as biocatalysts involved in biochemical reactions, play an important role in nutrient mineralization, decomposition of organic matter, and nutrient cycling (Chen et al., 2024; Liu et al., 2018). The DHA activity increased significantly in all three groups (244.00~3138.00% higher than the initial value) and continuously ( $P<0.05$ ) (Fig. S5A). Under flooding, microbial activity changed from aerobic to anaerobic, leading to a sharp decline in soil redox potential, accompanied by the stimulation of soil DHA (Sardans and Peñuelas, 2005). During operation, urease activity in CMFC showed a gradual increase (2.70~12.40% higher than day 0 from days 10~35), while it in OMFC and NMFC showed a slight decrease (6.10~7.10% lower than day 0 from days 5~35) (Fig. S5B). SMFC electric field and Fe(II) promote extracellular electron transfer (EET) (Chen et al., 2023a), which promotes the enrichment of ammonia-nitrogen transforming bacteria in soil could have caused the higher urease activity in CMFC than NMFC and OMFC ( $P<0.05$ ). Soil invertase activity decreased initially but increased later for CMFC and OMFC, but

showed an opposite trend for NMFC. After operation, CMFC had a significantly higher invertase activity than others ( $P<0.05$ ) (Fig. S5C). Soil ACP showed a similar trend with urease, with CMFC continuously increasing by 13.20~48.90% and considerably higher than OMFC and NMFC (Fig. S5D). The dynamic measurement of soil enzyme activity in SMFC helps us to understand and analyze the changing state of soil microecology.

### 3.5 SMFC operation reshaped soil microbial community

Microbial community structures in the electrodes were analyzed, which obtained 15 dominant phyla and 50 dominant genera ( $>1.00\%$ ). Overall, *Firmicutes* (73.93%), *Proteobacteria* (62.53%), and *Chloroflexi* (21.73%) were found the dominant phyla, while *Bacteroides* (21.48%), *Enterococcus* (17.26%), and *Hyphomicrobium* (15.34%) were the dominant genera.

The alpha diversity analysis indicated a significant difference in the microbial community among the samples (Fig. 5). The higher chao1 index in soils than the electrodes demonstrated higher microbial richness. Most of the alpha index in OMFC-A and OMFC-C were significantly higher than CMFC-A and CMFC-C, demonstrating a higher microbial richness and diversity in OMFC. The results indicated the different microbial evolution patterns in different electrodes and the selection effect of the electricity field during CMFC operation. The Venn diagram (Fig. S6) found no OTU coincidence among the samples, indicating their obvious specificity. In comparison, 2130 OTUs were shared by CMFC-S, OMFC-S, and NMFC-S, indicating the similarity of the soil microbial community (Fig. S6B). 45 OTUs were shared by Raw-A, CMFC-A, and OMFC-A, accounting for 45.92%, 1.95%, and 1.16%, respectively, indicating the successful colonization and development of the preloaded EABs.

-A present anode      -S present soil  
 -C present cathode    -Raw-A present anode before operation

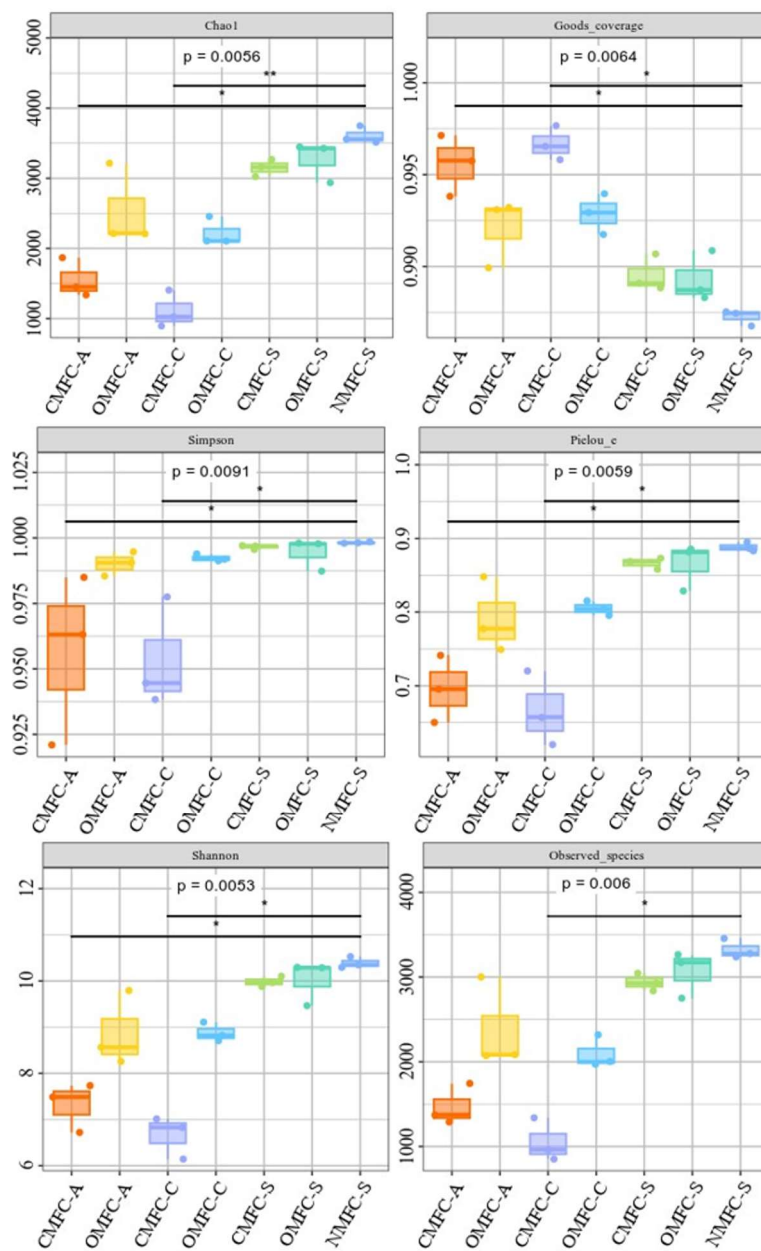


**Fig. 5** Alpha diversity analysis of the electrodes and soils

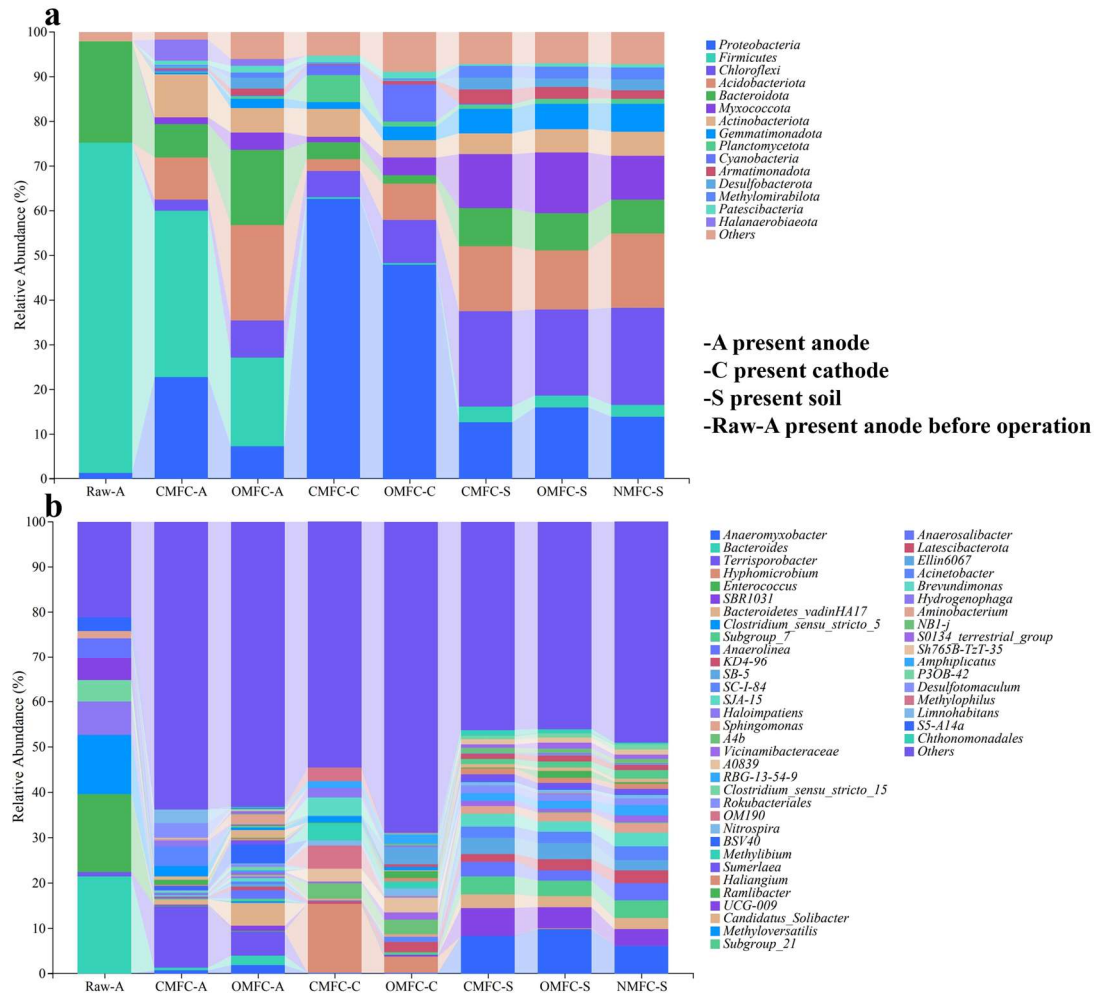


**Fig. 6** Microbial community structure is based on (a) the phylum level and (b) the genus level.

### 3.5.1 Soil microbial community reshaping on phylum level

At the phylum level (Fig. 6a), before the operation, the anode was dominated by *Firmicutes* (73.93%), *Bacteroidota* (22.74%), and *Proteobacteria* (1.27%). After the operation, *Firmicutes* and *Bacteroidota* decreased by 49.83% and 66.84% in CMFC-A, and 73.20% and 26.52% in OMFC-A, respectively. While *Proteobacteria* increased by 1 698.43% in CMFC-A and 475.59% in OMFC-A. Besides, many other phyla emerged, including *Acidobacteriota* (9.41%~21.40%), *Actinobacteriota* (0.23%~9.52%), *Halanaerobiaeota* (1.48%~4.77%), *Myxococcota* (1.51%~3.93%), *Chloroflexi* (0.01%~2.57%), indicating the increased microbial diversity, probably due to the penetration of soil indigenous microbe.

The cathode was free of microorganisms initially. However, many phyla were observed after the operation. The CMFC-C was dominated by *Proteobacteria* (62.53%), *Actinobacteriota* (6.24%), *Planctomycetota* (6.04%), *Chloroflexi* (5.88%), and *Bacteroidota* (3.81%), while OMFC-C was dominated by *Proteobacteria* (47.93%), *Chloroflexi* (9.75%), *Cyanobacteria* (8.30%), *Acidobacteriota* (8.01%), *Actinobacteriota* (3.97%), *Myxococcota* (3.92%), and *Gemmatimonadota* (2.87%). The *Proteobacteria* phylum was rich in EABs, its advantage in both electrodes of CMFC indicated that SMFC operation was favorable for EAB colonization and development. All the soils were dominated by *Chlorobacteria*, *Acidobacteria*, *Proteobacteria*, *Bacteroidetes*, and *Myxococcota*, and the difference was not significant.

### 3.5.2 Soil microbial community reshaping on genus level

At the genus level (Fig. 6b), MFC operation presented a selection effect, with *Terrisporobacter* increasing from 0.81% to 13.71% and *Bacteroides* decreasing from 12.48% to 0.53% in CMFC anode. Compared with the Raw-A, many EABs in CMFC-A decreased, including *Clostridium\_sensu\_stricto\_5* (from 12.99% to 0.05%), *Clostridium\_sensu\_stricto\_15* (from 4.70% to 0.47%), *Enterococcus* (from 17.26% to 0.03%) (Choi, 2022; Zhang et al., 2023).

However, the *Desulfotomaculum* in CMFC-A increased to 3.32% compared with 0.003% in the soil (CMFC-S). Besides, soil indigenous bacteria including *Ramlibacter*, *Methyloversatilis*, and *Acinetobacter* colonized in the anode and elevated by 4.89~1 579.00 fold compared with soil. Nevertheless, multiple dominant genera in the soils decreased in CMFC-A than in OMFC-A. For example, *SBR1031*, *Bacteroidetes\_vadinHA17*, and *Anaerolinea* were significantly increased in soil, but less in CMFC-A and OMFC-A. The electric field action to a certain extent helped the anode to resist

external microbial intrusion to ensure the stability of the anodic microbial community.

During operation, the prolonged interaction between the soil and water phases resulted in the gradually evolving unique biofilm structure of the cathode. For instance, *Hyphomicrobium* (3.56~15.34% in soils), an aerobic chemoheterotroph capable of degrading a wide range of organics, accounted for 15.34% and 3.56% of CMFC-C and OMFC-C, respectively (He et al., 2019). *Hydrogenophaga*, a gram-negative bacteria capable of denitrification and Cr(VI) reduction, accounted for 2.07% of CMFC-C (Wang et al., 2022). Meanwhile, the SMFC operation caused the enrichment of several resistant bacteria. *Subgroup\_7*, a typical HM-tolerant bacterium (Li et al., 2023a), was enriched in both cathode and soil. *Acinetobacter* and *Limnohabitans*, also tolerators that carry HRGs and ARGs, were found 4.31% and 3.03% in CMFC-A (Dahal et al., 2023; Zhang et al., 2021).

The increase of iron in soil and water due to the use of Fe<sub>3</sub>O<sub>4</sub> as cathode catalyst may be responsible for the enrichment of *Terrisporobacter* and *Anaeromyxobacter* in the CMFC-A and OMFC-A. They were found closely associated with Fe<sup>3+</sup> reduction to gain energy in various environments (Lin et al., 2007; Wang et al., 2020b).

### 3.5.3 Soil metal resistance gene variation

Under Cr(VI) stress, certain microbes would utilize pathways like specific or non-specific Cr(VI) reduction, free radical detoxification, DNA damage repair, etc. to survive in toxic environments (Morais et al., 2011). Using qPCR analysis, the abundance of typical HRGs and MGEs in the anodic soils was determined (Fig. 7a), among which *chrA*, *chrB*, and *chrR*, are typical HRGs involved in Cr response, while *IntI*, *tnpA02*, and *tnpA05* are common mobile genetic elements (MGEs) that varied greatly during operation ( $P<0.05$ ). Compared with OMFC and NMFC, *chrA* in CMFC increased by 237.83% and

3414.34%, *chrB* by 141.52% and 153.63%, *chrR* by 221.86% and 839.41%, *IntI* by 151.77% and 167.91%, *tnpA02* by 331.86% and 1118.97%, and *tnpA05* by 416.91% and 99.54%. Changes in soil resistance characteristics during SMFC operation may be directly or indirectly caused by environmental factors and resistant microbial communities.

The elevation of HRGs and MGEs could be due to the enrichment of multiple metal-resistant bacteria (MRB) such as *Acinetobacter*, *Limnohabitans*, and *Brevundimonas*. Moreover, the anodic *Desulfotomaculum*, which accounted for 3.23% of CMFC-A, is a typical sulfate-reducing bacterium (SRB) that produces H<sub>2</sub>S, a natural signaling molecule that contributes to tolerance triggering, maintenance, and diffusion through community sensing, which facilitates HRG elevation through HGT (Shatalin et al., 2021). Besides, Cr(VI) reducing bacteria like *Hydrogenophaga* (1.31% in CMFC-A) may also up-regulate the Cr reductase gene *chrR* (Sundarraj et al., 2023).

Furthermore, pH changes may also affect soil resistance characteristics. Liu et al. (2023c) observed the abundance of multidrug efflux pump genes in the acid soil was significantly positively correlated with soil acidity. The intensified proton generation and accumulation in CMFC could have led to the HRG elevation. In addition, HMs toxicity exerts direct selective pressure, which affects microbial community structure and their function, leading to the thriving of tolerators like *Desulfotomaculum sp*, *Hydrogenophaga*, and *Methylophilus* (Hernández-Ramírez et al., 2018), hence the spontaneous HRG elevation (Wang et al., 2023c).

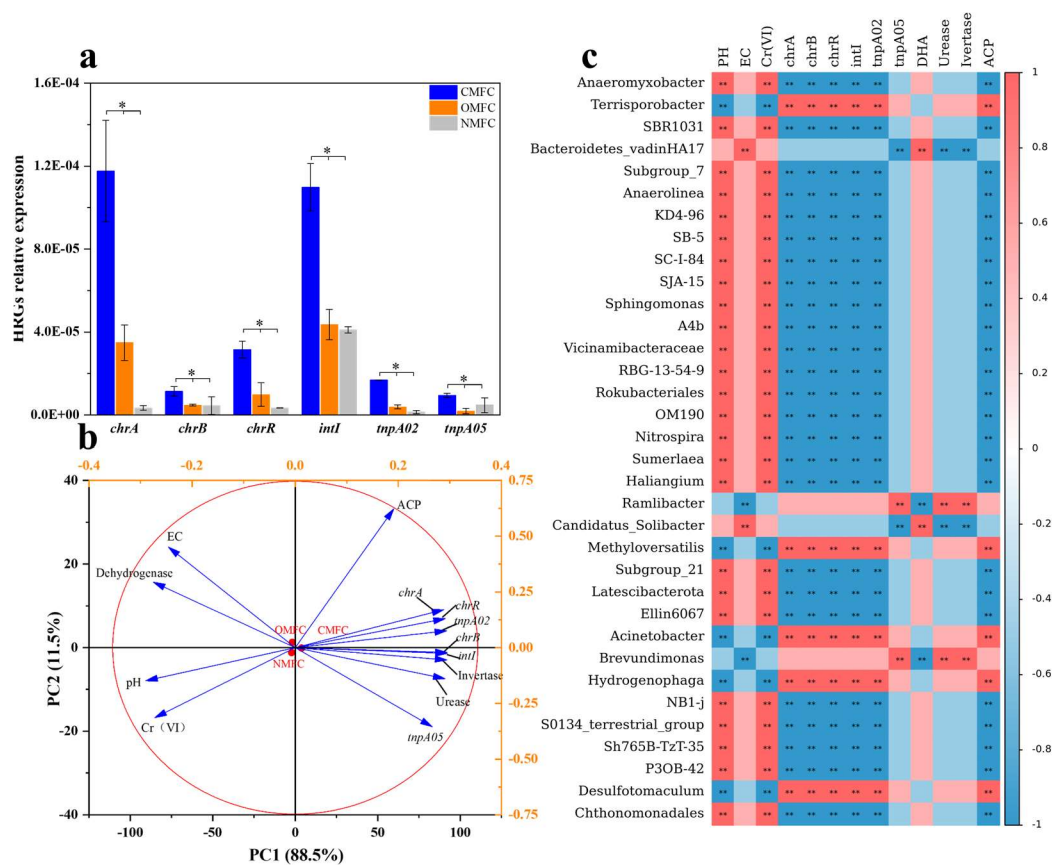


**Fig. 7** HRG variation and correlation analysis of dominant bacteria, HRG, and soil enzymatic activity. (a) qPCR results of HRG changes in soil around anode-soil after SMFC operation (*chrA*, *chrB*, *chrR*, *intI*, *tnpA02*, *tnpA05*). Different letters denote significant differences among treatments ( $P < 0.05$ ); (b) principal component analysis (PCA) of SMFC soil physicochemical properties with Enzyme activity, HRGs, and native bacterial genera and (c) Spearman's correlation heatmap (mean relative abundance > 1%). \*  $P < 0.05$ , according to LSD test (mean  $\pm$  S.E.,  $n = 3$ ); \*\*  $P < 0.01$ .

### 3.6 Correlation analysis

To visually analyze the correlation between bacterial communities and environmental factors, spearman correlation analysis and principal component analysis (PCA) were conducted (Fig. 7). Spearman correlation analysis (Fig. 7c) isolated four main bacterial genera clusters, which further revealed the correlation of environmental factors (pH, EC), soil enzyme activities (DHA, Urease, Invertase, ACP),



Cr(VI), and HRGs (*chrA*, *chrB*, *intI*, *tnpA02*, *tnpA05*) with the microbial community.

Cluster 1 (*Terrisporobacter*, *Methyloversatilis*, *Acinetobacter*, *Hydrogenophaga*, and *Desulfotomaculum*) was positively correlated with HRGs (*chrA*, *chrB*, *intI*, *tnpA02*) and ACP ( $P<0.01$ ), but negatively correlated with pH and Cr(VI) ( $P<0.01$ ), suggesting they may contribute to HGT and HRGs enrichment.

Cluster 2 (*Anaeromyxobacter*, *Subgroup\_7*, *Anaerolinea*, *SB-5*, *Sphingomonas*, etc.) was negatively correlated ( $P<0.01$ ) with HRGs (*chrA*, *chrB*, *intI*, *tnpA02*) and ACP, but positively correlated with pH and Cr(VI) ( $P<0.01$ ). Cluster 3 (*Bacteroidetes\_vadinHA17* and *Candidatus\_Solibacter*) was positively correlated ( $P<0.01$ ) with soil EC and DHA. Cluster 4 (*Ramlibacter*, and *Brevundimonas*) were positively correlated with urease and invertase but negatively correlated with EC.

PCA analysis (Fig. 7b) also indicated a close correlation between environmental factors, in which soil pH, EC, Cr(VI) concentration, and DHA were positively correlated with each other but negatively correlated with urease, ACP, invertase, and HRGs. Especially, Cr(VI) was significantly negatively correlated with HRGs ( $P<0.01$ ), which could be partially explained by the tolerators thriving and Cr(VI) reduction during SMFC operation.

#### 4. Discussion

In this study, Cr(VI) reduction, microbial community variation, and HRG fate in SMFC were investigated for the first time. The results proved that SMFC was an effective method to eliminate Cr(VI) (93.76%), immobilize Cr (97.44%), and generate electricity (0.97 V).

Microorganisms have developed efficient detoxification strategies to counteract the toxic effects of heavy metal stress (Rouch et al., 1995; Tan et al., 2020). In the SMFC system, Cr(VI) reduction was a synergic result of adsorption/biosorption (including the adsorption of anode and cathode materials,

surface catalyst adsorption, and microbial membrane adsorption), bioelectrochemistry reduction, and microbial reduction (including intracellular sequestration, export, reduced permeability, extracellular sequestration, and extracellular detoxification) (Fig. 8). The preloading of  $\text{Fe}_3\text{O}_4$  and EABs on the electrodes significantly improved Cr(VI) reduction and power generation by accelerating SMFC stabilization. The detailed explanation is as follows:

The electricity-producing process of SMFC can inhibit HMs' release and migration in soil (Zhu et al., 2019; Feng et al., 2024). In this study, Cr forms changed greatly from acid-soluble to a more stable residual fraction with low toxicity. The  $\text{Fe}_3\text{O}_4$ -modified cathode not only directly adsorbs or reduces Cr(VI) due to the high specific area and ferrous iron, but also enhances the electrochemical effect of the system. The electrons derived from anodic microbial metabolism can directly reduce Cr(VI) in the soil to Cr(III), while part of them is transmitted to the cathode, where Cr(VI) in the overlying water compete with oxygen as electron acceptors and complete the current loop (Thapa et al., 2022).

In addition, microorganisms can also directly or indirectly reduce or fix Cr. Biosorption, sulfide, and hydroxide precipitation are the main immobilization mechanisms of HMs by microorganisms (Ma et al., 2024). For example, *Desulfotomaculum* sp., a typical SRB, enriched to 3.23% in CMFC-A, may produce sulfide ions by reducing alienated sulfate, thus forming highly insoluble metal sulfide to fix Cr through microorganism-induced sulfide precipitation (MISP). *Hydrogenophaga*, which dominated in both electrodes, was a known Cr-reducing bacteria. Some of iron-reducing bacteria present in this study (e.g., *Anaeromyxobacter* and *Terrisporobacter*) may also contribute to Cr(VI) reduction by participating in the Fe cycle through EET, while the ferrous iron reduces Cr(VI). Additionally, the CMFC in this work contains many genera capable of transforming nitrogen. For example, *Hyphomicrobium* dominated in

CMFC-C (15.34%), a typical denitrifying bacterium, can effectively reduce nitrate and nitrite (Ernst et al., 2021). *Methylophilus* accounted for 2.93% of CMFC-A but was much lower in other groups, which is a methylotrophic microorganism (Yang et al., 2020). The bacteria mentioned above were found with high urease-producing ability, whose enrichment not only improves soil urease activity and nutrient cycling but also immobilizes Cr through microorganism-induced carbonate precipitation (MICP) (Qian et al., 2017).

In addition to the reduction of Cr during SMFC operation, under electrochemical selection and HMs stress, the microbial community gradually evolved with higher richness and diversity, along with the HRG enrichment and nutrient cycling variation. Firstly, some soil indigenous bacteria were much lower in CMFC-A than OMFC-A, indicating the electric field contributed to the anode stability by preventing external bacteria intrusion and is less vulnerable to environmental fluctuations. The microbial community change is significantly related to HRG enrichment. Many EABs and MRBs are significantly enriched. For example, *Desulfotomaculum*, an SRB with a dual role of electroproduction and HMs reduction (Jiang et al., 2020; Yin et al., 2021). Other examples also include cumulative-resistant bacteria like *Acinetobacter* and *Limnohabitans* which are only enriched in the CMFC-A (Dahal et al., 2023; Al-Jabri et al., 2018). Their enrichment directly causes vertical gene transfer and HRG elevation. The Cr forms, soil physicochemical properties, soil enzyme activities, and microecological structure mirrored each other, helping to understand Cr transformation patterns and target the key factors affecting metal resistance changes.

HMs existence in soil can induce HGT occurrence and cause ARG elevation, which has become a major concern (Chen et al., 2023b; Fu et al., 2023). Sub-lethal levels of metal ions can increase mutation

rates and enrich de novo mutants with significant resistance to multiple antibiotics (Li et al., 2019). This study focused on the toxic alleviation of a single HM (Cr) in SMFC, during which tolerator accumulation caused considerable HRG enrichment. SMFC is an eco-friendly and cost-effective technology for the in situ bioremediation of contaminated soil/sediment and powering environmental sensors in remote areas. It has the potential to be used as a novel early warning system for soil environmental hazards. Nevertheless, before the commercialization of large-scale applications in the field, significant efforts should be made to reveal the HRG enrichment mechanism during SMFC operation and pay attention to ARG change under HMs contamination or HMs-antibiotic co-contamination.

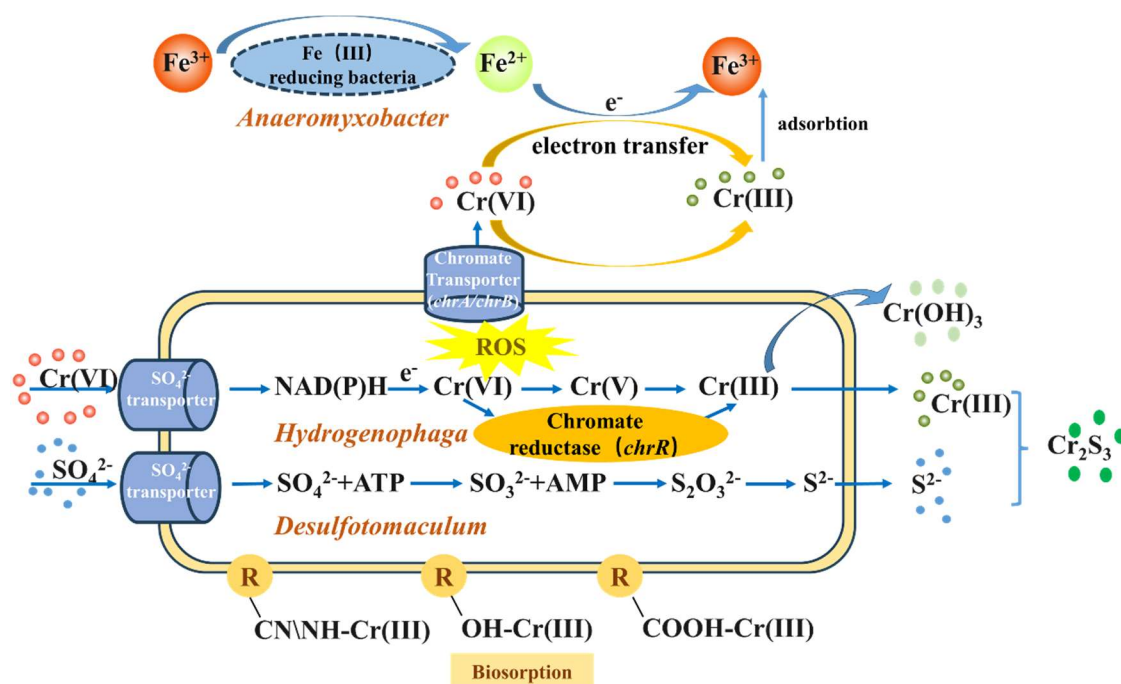


**Fig. 8** Cr(VI) reduction mechanism during SMFC operation

## 5. Conclusion

During SMFC operation, the close interaction among the soil physicochemical properties, enzyme activities, resistance genes, and microbial community structure determined the performance. The pre-loading of  $Fe_3O_4$  in the cathode and EAB in the anode greatly contributed to power production and Cr(VI)

elimination. Anodic microbial metabolism, cathodic redox, and the MFC electric field reduced or immobilized Cr(VI) to eliminate its risk. The enrichment of multiple MRBs, such as *Acinetobacter*, *Limnohabitans*, and *Desulfotomaculum*, resulted in HRG elevation, which contributes to microbial adaptation and function but brings concerns for future application. This study provides a reference for the remediation of HM-contaminated soil using MFC, which is conducive to promoting the practical application of bioelectrochemical technology in the field.

#### **Author contribution:**

HN: Conceptualization, Investigation, and Writing; XL: Investigation, Visualization; PL: Investigation, Visualization; HQ: Methodology; LJ: Writing-review and editing; SM: Writing-review and editing; MW: Writing-review; FX: Funding acquisition, Supervision; HX: Funding acquisition, Supervision; CW: Funding acquisition, Supervision.

#### **Acknowledgments**

This work was financially supported by the Sichuan Science and Technology Program (2024NSFSC0384, 2025ZNSFSC0200 and 25NSFSC2362), the Government Guides Local Science and Technology Development Project of the Tibetan Autonomous Region of China (XZ202401YD0001), the China Postdoctoral Science Foundation (2022M712630), and the National Natural Science Foundation of China (No. 42207021). We thank Dr. Weizhen Fang from the Analysis & Testing Center and Dr. Cuijuan Wang from the School of Chemistry, Southwest Jiaotong University, for the technical support. We thank Lijuan Zhang from SCI-Go ([www.sci-go.com](http://www.sci-go.com)) for the XPS analysis.

## Declaration of interests

The authors declare that they have no known competing financial interests or personal relationships that could have appeared to influence the work reported in this paper.

## Reference

- AL-Jabri, Z., Zamudio, R., Horvath-Papp, E., Ralph, J. D., AL-Muharrami, Z., Rajakumar, K., and Oggioni, M. R.: Integrase-Controlled Excision of Metal-Resistance Genomic Islands in *Acinetobacter baumannii*, *Genes*, 9, 366, <https://doi.org/10.3390/genes9070366>, 2018.
- Ashbolt Nicholas, J., Amézquita, A., Backhaus, T., Borriello, P., Brandt Kristian, K., Collignon, P., Coors, A., Finley, R., Gaze William, H., Heberer, T., Lawrence John, R., Larsson, D. G. J., McEwen Scott, A., Ryan James, J., Schönfeld, J., Silley, P., Snape Jason, R., Van den Eede, C., and Topp, E.: Human Health Risk Assessment (HHRA) for Environmental Development and Transfer of Antibiotic Resistance, *Environ. Health Perspect.*, 121, 993-1001, <https://doi.org/10.1289/ehp.1206316>, 2013.
- Bokulich, N. A., Kaehler, B. D., Rideout, J. R., Dillon, M., Bolyen, E., Knight, R., Huttley, G. A., and Gregory Caporaso, J.: Optimizing taxonomic classification of marker-gene amplicon sequences with QIIME 2's q2-feature-classifier plugin, *Microbiome*, 6, 90, <https://doi.org/10.1186/s40168-018-0470-z>, 2018.
- Chen, C., Fang, Y., and Zhou, D.: Selective pressure of PFOA on microbial community: Enrichment of denitrifiers harboring ARGs and the transfer of ferric-electrons, *Water Res.*, 233, 119813, <https://doi.org/10.1016/j.watres.2023.119813>, 2023a.
- Chen, M., Cai, Y., Li, G., Zhao, H., and An, T.: The stress response mechanisms of biofilm formation under sub-lethal photocatalysis, *Appl. Catal., B*, 307, 121200, <https://doi.org/10.1016/j.apcatb.2022.121200>, 2022a.
- Chen, P., Zhang, T., Chen, Y., Ma, H., Wang, Y., Liu, W., Wang, Y., Zhou, G., Qing, R., Zhao, Y., Xu, H., Hao, L., Wang, C., and Xu, F.: Integrated Chamber-free Microbial Fuel Cell for Wastewater Purification and Bioenergy Generation, *Chem. Eng. J.*, 136091, <https://doi.org/10.1016/j.cej.2022.136091>, 2022b.
- Chen, X., Du, Z., Song, X., Wang, L., Wei, Z., Jia, L., and Zhao, R.: Evaluating the occurrence frequency of horizontal gene transfer induced by different degrees of heavy metal stress, *J. Cleaner Prod.*, 382, 135371, <https://doi.org/10.1016/j.jclepro.2022.135371>, 2023b.
- Chen, Y., Zuo, M., Yang, D., He, Y., Wang, H., Liu, X., Zhao, M., Xu, L., Ji, J., Liu, Y., and Gao, T.: Synergistically Effect of Heavy Metal Resistant Bacteria and Plants on Remediation of Soil Heavy Metal Pollution, *Water, Air, Soil Pollut.*, 235, 296, <https://doi.org/10.1007/s11270-024-07100-w>, 2024.
- Choi, S.: Electrogenic Bacteria Promise New Opportunities for Powering, Sensing, and

499 Synthesizing, Small, 18, 2107902, <https://doi.org/10.1002/sml.202107902>,  
 500 2022.  
 501 Coetzee, J. J., Bansal, N., and Chirwa, E. M. N.: Chromium in Environment, Its Toxic  
 502 Effect from Chromite-Mining and Ferrochrome Industries, and Its Possible  
 503 Bioremediation, Exposure and Health, 12, 51-62,  
 504 <https://doi.org/10.1007/s12403-018-0284-z>, 2020.  
 505 Cong, Y., Shen, L., Wang, B., Cao, J., Pan, Z., Wang, Z., Wang, K., Li, Q., and Li, X.:  
 506 Efficient removal of Cr(VI) at alkaline pHs by sulfite/iodide/UV: Mechanism  
 507 and modeling, Water Res., 222, 118919,  
 508 <https://doi.org/10.1016/j.watres.2022.118919>, 2022.  
 509 Dahal, U., Paul, K., and Gupta, S.: The multifaceted genus *Acinetobacter*: from  
 510 infection to bioremediation, J. Appl. Microbiol., 134,  
 511 <https://doi.org/10.1093/jambio/lxad145>, 2023.  
 512 Deng, Y., Jiang, Y.-H., Yang, Y., He, Z., Luo, F., and Zhou, J.: Molecular ecological  
 513 network analyses, BMC Bioinformatics, 13, 113,  
 514 <https://doi.org/10.1186/1471-2105-13-113>, 2012.  
 515 Dimova, M., Iutynska, G., Yamborko, N., Dordevic, D., and Kushkevych, I.: Possible  
 516 Processes and Mechanisms of Hexachlorobenzene Decomposition by the  
 517 Selected *Comamonas testosteroni* Bacterial Strains, Processes, 10, 2170;  
 518 <https://doi.org/10.3390/pr10112170>, 2022.  
 519 Ernst, C., Kayastha, K., Koch, T., Venceslau, S. S., Pereira, I. A. C., Demmer, U., Ermler,  
 520 U., and Dahl, C.: Structural and spectroscopic characterization of a HdrA-like  
 521 subunit from *Hyphomicrobium denitrificans*, The FEBS Journal, 288, 1664-  
 522 1678, <https://doi.org/10.1111/febs.15505>, 2021.  
 523 Fan, C., Qian, J., Yang, Y., Sun, H., Song, J., and Fan, Y.: Green ceramsite production  
 524 via calcination of chromium contaminated soil and the toxic Cr(VI)  
 525 immobilization mechanisms, J. Cleaner Prod., 315, 128204,  
 526 <https://doi.org/10.1016/j.jclepro.2021.128204>, 2021.  
 527 Fan, Q., Fan, L., Quach, W.-M., Zhang, R., Duan, J., and Sand, W.: Application of  
 528 microbial mineralization technology for marine concrete crack repair: A  
 529 review, J. Building Engineering, 69, 106299,  
 530 <https://doi.org/10.1016/j.jobbe.2023.106299>, 2023.  
 531 Farkas, D., Proctor, K., Kim, B., Avignone Rossa, C., Kasprzyk-Hordern, B., and Di  
 532 Lorenzo, M.: Assessing the impact of soil microbial fuel cells on atrazine  
 533 removal in soil, J. Hazard. Mater., 478, 135473,  
 534 <https://doi.org/10.1016/j.jhazmat.2024.135473>, 2024.  
 535 Faust, K. and Raes, J.: Microbial interactions: from networks to models, Nat. Rev.  
 536 Microbiol., 10, 538-550, <https://doi.org/10.1038/nrmicro2832>, 2012.  
 537 Feng, H., Jin, A., Yin, X., Hong, Z., Ding, Y., Zhao, N., Chen, Y., and Zhang, Y.:  
 538 Enhancing biocathode denitrification performance with nano-Fe<sub>3</sub>O<sub>4</sub> under  
 539 polarity period reversal, Environ. Res., 241, 117641,  
 540 <https://doi.org/10.1016/j.envres.2023.117641>, 2024.

- Fu, Y., Zhu, Y., Dong, H., Li, J., Zhang, W., Shao, Y., and Shao, Y.: Effects of heavy metals and antibiotics on antibiotic resistance genes and microbial communities in soil, *Process Saf. Environ. Prot.*, 169, 418-427, <https://doi.org/10.1016/j.psep.2022.11.020>, 2023.
- Guo, S., Xiao, C., Zhou, N., and Chi, R.: Speciation, toxicity, microbial remediation and phytoremediation of soil chromium contamination, *Environ. Chem. Lett.*, 19, 1413-1431, <https://doi.org/10.1007/s10311-020-01114-6>, 2021.
- Gupta, S., Patro, A., Mittal, Y., Dwivedi, S., Saket, P., Panja, R., Saeed, T., Martínez, F., and Yadav, A. K.: The race between classical microbial fuel cells, sediment-microbial fuel cells, plant-microbial fuel cells, and constructed wetlands-microbial fuel cells: Applications and technology readiness level, *Sci. Total Environ.*, 879, 162757, <https://doi.org/10.1016/j.scitotenv.2023.162757>, 2023.
- Gustave, W., Yuan, Z.-F., Li, X., Ren, Y.-X., Feng, W.-J., Shen, H., and Chen, Z.: Mitigation effects of the microbial fuel cells on heavy metal accumulation in rice (*Oryza sativa* L.), *Environ. Pollut.*, 260, 113989, <https://doi.org/10.1016/j.envpol.2020.113989>, 2020.
- Hamdan, H. Z. and Salam, D. A.: Sediment microbial fuel cells for bioremediation of pollutants and power generation: a review, *Environ. Chem. Lett.*, 21, 2761-2787, <https://doi.org/10.1007/s10311-023-01625-y>, 2023.
- He, Q., Gui, J., Liu, D., Li, X., Li, P., and Quan, S.: Research progress of soil property's changes and its impacts on soil cadmium activity in flooded paddy field, *J. Agro-Environ. Sci.*, 35, 2260-2268, <https://doi.org/10.11654/jaes.2016-0892>, 2016.
- He, S., Guo, H., He, Z., Yang, C., Yu, T., Chai, Q., and Lu, L.: Interaction of *Lolium perenne* and *Hyphomicrobium* sp. GHH enhances the removal of 17 $\alpha$ -ethinyestradiol (EE2) from soil, *J. Soils Sed.*, 19, 1297-1305, <https://doi.org/10.1007/s11368-018-2116-y>, 2019.
- Hernández-Ramírez, K. C., Reyes-Gallegos, R. I., Chávez-Jacobo, V. M., Díaz-Magaña, A., Meza-Carmen, V., and Ramírez-Díaz, M. I.: A plasmid-encoded mobile genetic element from *Pseudomonas aeruginosa* that confers heavy metal resistance and virulence, *Plasmid*, 98, 15-21, <https://doi.org/10.1016/j.plasmid.2018.07.003>, 2018.
- Irankhah, S., Abdi Ali, A., Mallavarapu, M., Soudi, M. R., Subashchandrabose, S., Gharavi, S., and Ayati, B.: Ecological role of *Acinetobacter calcoaceticus* GSN3 in natural biofilm formation and its advantages in bioremediation, *Biofouling*, 35, 377-391, <https://doi.org/10.1080/08927014.2019.1597061>, 2019.
- Jia, J., Bai, J., Xiao, R., Tian, S., Wang, D., Wang, W., Zhang, G., Cui, H., and Zhao, Q.: Fractionation, source, and ecological risk assessment of heavy metals in cropland soils across a 100-year reclamation chronosequence in an estuary, South China, *Sci. Total Environ.*, 807, 151725, <https://doi.org/10.1016/j.scitotenv.2021.151725>, 2022.



- Jiang, Y., Shang, Y., Gong, T., Hu, Z., Yang, K., and Shao, S.: High concentration of  $Mn^{2+}$  has multiple influences on aerobic granular sludge for aniline wastewater treatment, *Chemosphere*, 240, 124945, <https://doi.org/10.1016/j.chemosphere.2019.124945>, 2020.
- Kim, C., Lee, C. R., Song, Y. E., Heo, J., Choi, S. M., Lim, D.-H., Cho, J., Park, C., Jang, M., and Kim, J. R.: Hexavalent chromium as a cathodic electron acceptor in a bipolar membrane microbial fuel cell with the simultaneous treatment of electroplating wastewater, *Chem. Eng. J.*, 328, 703-707, <https://doi.org/10.1016/j.cej.2017.07.077>, 2017.
- Li, C., Huang, H., Gu, X., Zhong, K., Yin, J., Mao, J., Chen, J., and Zhang, C.: Accumulation of heavy metals in rice and the microbial response in a contaminated paddy field, *J. Soils Sed.*, <https://doi.org/10.1007/s11368-023-03643-3>, 2023a.
- Li, X., Gu, A. Z., Zhang, Y., Xie, B., Li, D., and Chen, J.: Sub-lethal concentrations of heavy metals induce antibiotic resistance via mutagenesis, *J. Hazard. Mater.*, 369, 9-16, <https://doi.org/10.1016/j.jhazmat.2019.02.006>, 2019.
- Li, Y., Lin, J., Wu, Y., Jiang, S., Huo, C., Liu, T., Yang, Y., and Ma, Y.: Transformation of exogenous hexavalent chromium in soil: Factors and modelling, *J. Hazard. Mater.*, 480, 135799, <https://doi.org/10.1016/j.jhazmat.2024.135799>, 2024.
- Li, Y., Chen, Y., Chen, Y., Qing, R., Cao, X., Chen, P., Liu, W., Wang, Y., Zhou, G., Xu, H., Hao, L., Wang, C., Li, S., Zhu, Y., Haderlein, S., and Xu, F.: Fast deployable real-time bioelectric dissolved oxygen sensor based on a multi-source data fusion approach, *Chem. Eng. J.*, 475, 146064, <https://doi.org/10.1016/j.cej.2023.146064>, 2023b.
- Lin, B., Hyacinthe, C., Bonneville, S., Braster, M., Van Cappellen, P., and Röling, W. F. M.: Phylogenetic and physiological diversity of dissimilatory ferric iron reducers in sediments of the polluted Scheldt estuary, Northwest Europe, *Environ. Microbiol.*, 9, 1956-1968, <https://doi.org/10.1111/j.1462-2920.2007.01312.x>, 2007.
- Liu, H., Xu, F., Xie, Y., Wang, C., Zhang, A., Li, L., and Xu, H.: Effect of modified coconut shell biochar on availability of heavy metals and biochemical characteristics of soil in multiple heavy metals contaminated soil, *Sci. Total Environ.*, 645, 702-709, <https://doi.org/10.1016/j.scitotenv.2018.07.115>, 2018.
- Liu, S., Feng, Y., and Li, H.: Degradation mechanism of saliferous compounding heavy metals-organic wastewater by manganese and iron cycling in the microbial fuel cell, *Chem. Eng. J.*, 473, 145389, <https://doi.org/10.1016/j.cej.2023.145389>, 2023a.
- Liu, S., Pu, S., Deng, D., Huang, H., Yan, C., Ma, H., and Razavi, B. S.: Comparable effects of manure and its biochar on reducing soil Cr bioavailability and narrowing the rhizosphere extent of enzyme activities, *Environ. Int.*, 134, 105277, <https://doi.org/10.1016/j.envint.2019.105277>, 2020.
- Liu, X.-C., Zhang, K.-X., Song, J.-S., Zhou, G.-N., Li, W.-Q., Ding, R.-R., Wang, J.,

- Zheng, X., Wang, G., and Mu, Y.: Tuning Fe<sub>3</sub>O<sub>4</sub> for sustainable cathodic heterogeneous electro-Fenton catalysis by acetylated chitosan, *Proc. Natl. Acad. Sci.*, 120, e2213480120, <https://doi.org/10.1073/pnas.2213480120>, 2023b.
- Liu, Z., Zhao, Y., Zhang, B., Wang, J., Zhu, L., and Hu, B.: Deterministic Effect of pH on Shaping Soil Resistome Revealed by Metagenomic Analysis, *Environ. Sci. Technol.*, 57, 985-996, <https://doi.org/10.1021/acs.est.2c06684>, 2023c.
- Ma, S., Mao, S., Shi, J., Zou, J., Zhang, J., Liu, Y., Wang, X., Ma, Z., and Yu, C.: Exploring the synergistic interplay of sulfur metabolism and electron transfer in Cr(VI) and Cd(II) removal by *Clostridium thiosulfatireducens*: Genomic and mechanistic insights, *Chemosphere*, 352, 141289, <https://doi.org/10.1016/j.chemosphere.2024.141289>, 2024.
- Mandal, S., Sarkar, B., Bolan, N., Ok, Y. S., and Naidu, R.: Enhancement of chromate reduction in soils by surface modified biochar, *J. Environ. Manage.*, 186, 277-284, <https://doi.org/10.1016/j.jenvman.2016.05.034>, 2017.
- Men, C., Liu, R., Xu, F., Wang, Q., Guo, L., and Shen, Z.: Pollution characteristics, risk assessment, and source apportionment of heavy metals in road dust in Beijing, China, *Sci. Total Environ.*, 612, 138-147, <https://doi.org/10.1016/j.scitotenv.2017.08.123>, 2018.
- Morais, P. V., Branco, R., and Francisco, R.: Chromium resistance strategies and toxicity: what makes *Ochrobactrum tritici* 5bvl1 a strain highly resistant, *BioMetals*, 24, 401-410, <https://doi.org/10.1007/s10534-011-9446-1>, 2011.
- Morales-Benítez, I., Montoro-Leal, P., García-Mesa, J. C., López Guerrero, M. M., and Vereda Alonso, E.: New magnetic chelating sorbent for chromium speciation by magnetic solid phase extraction on-line with inductively coupled plasma optical emission spectrometry, *Talanta*, 256, 124262, <https://doi.org/10.1016/j.talanta.2023.124262>, 2023.
- Qian, X., Fang, C., Huang, M., and Achal, V.: Characterization of fungal-mediated carbonate precipitation in the biomineralization of chromate and lead from an aqueous solution and soil, *J. Cleaner Prod.*, 164, 198-208, <https://doi.org/10.1016/j.jclepro.2017.06.195>, 2017.
- Rani, L., Kaushal, J., and Lal Srivastav, A.: Biochar as sustainable adsorbents for chromium ion removal from aqueous environment: a review, *Biomass Convers. Biorefin.*, <https://doi.org/10.1007/s13399-022-02784-8>, 2022.
- Rouch, D. A., Lee, B. T. O., and Morby, A. P.: Understanding cellular responses to toxic agents: a model for mechanism-choice in bacterial metal resistance, *J. Ind. Microbiol.*, 14, 132-141, <https://doi.org/10.1007/BF01569895>, 1995.
- Sardans, J. and Peñuelas, J.: Drought decreases soil enzyme activity in a Mediterranean *Quercus ilex* L. forest, *Soil Biol. Biochem.*, 37, 455-461, <https://doi.org/10.1016/j.soilbio.2004.08.004>, 2005.
- Shatalin, K., Nuthanakanti, A., Kaushik, A., Shishov, D., Peselis, A., Shamovsky, I., Pani, B., Lechpammer, M., Vasilyev, N., Shatalina, E., Rebatchouk, D.,

- Mironov, A., Fedichev, P., Serganov, A., and Nudler, E.: Inhibitors of bacterial H<sub>2</sub>S biogenesis targeting antibiotic resistance and tolerance, *Science*, 372, 1169-1175, <https://doi.org/10.1126/science.abd8377>, 2021.
- Sundarraaj, S., Sudarmani, D. N. P., Samuel, P., and Sevarkodiyone, S. P.: Bioremediation of hexavalent chromium by transformation of *Escherichia coli* DH5 $\alpha$  with chromate reductase (*ChrR*) genes of *Pseudomonas putida* isolated from tannery effluent, *J. Appl. Microbiol.*, 134, lxac019, <https://doi.org/10.1093/jambio/lxac019>, 2023.
- Tan, H., Wang, C., Zeng, G., Luo, Y., Li, H., and Xu, H.: Bioreduction and biosorption of Cr(VI) by a novel *Bacillus* sp. CRB-B1 strain, *J. Hazard. Mater.*, 386, 121628, <https://doi.org/10.1016/j.jhazmat.2019.121628>, 2020.
- Thapa, B. S., Kim, T., Pandit, S., Song, Y. E., Afsharian, Y. P., Rahimnejad, M., Kim, J. R., and Oh, S.-E.: Overview of electroactive microorganisms and electron transfer mechanisms in microbial electrochemistry, *Bioresour. Technol.*, 347, 126579, <https://doi.org/10.1016/j.biortech.2021.126579>, 2022.
- van Hoek, A. H., Mevius, D., Guerra, B., Mullany, P., Roberts, A. P., and Aarts, H. J.: Acquired Antibiotic Resistance Genes: An Overview, *Front. Microbiol.*, 2, <https://doi.org/10.3389/fmicb.2011.00203>, 2011.
- Wang, C., Zhou, Z., Liu, H., Li, J., Wang, Y., and Xu, H.: Application of acclimated sewage sludge as a bio-augmentation/bio-stimulation strategy for remediating chlorpyrifos contamination in soil with/without cadmium, *Sci. Total Environ.*, 579, 657-666, <https://doi.org/10.1016/j.scitotenv.2016.11.044>, 2017.
- Wang, C., Li, Y. Z., Tan, H., Zhang, A. K., Xie, Y. L., Wu, B., and Xu, H.: A novel microbe consortium, nano-visible light photocatalyst and microcapsule system to degrade PAHs, *Chem. Eng. J.*, 359, 1065-1074, <https://doi.org/10.1016/j.cej.2018.11.077>, 2019.
- Wang, C., Tan, H., Li, H., Xie, Y., Liu, H., Xu, F., and Xu, H.: Mechanism study of Chromium influenced soil remediated by an uptake-detoxification system using hyperaccumulator, resistant microbe consortium, and nano iron complex, *Environ. Pollut.*, 257, 113558, <https://doi.org/10.1016/j.envpol.2019.113558>, 2020a.
- Wang, C., Jia, Y., Li, J., Wang, Y., Niu, H., Qiu, H., Li, X., Fang, W., and Qiu, Z.: Effect of bioaugmentation on tetracyclines influenced chicken manure composting and antibiotics resistance, *Sci. Total Environ.*, 867, 161457, <https://doi.org/10.1016/j.scitotenv.2023.161457>, 2023a.
- Wang, C., Jia, Y., Li, J., Li, P., Wang, Y., Yan, F., Wu, M., Fang, W., Xu, F., and Qiu, Z.: Influence of microbial augmentation on contaminated manure composting: metal immobilization, matter transformation, and bacterial response, *J. Hazard. Mater.*, 441, 129762, <https://doi.org/10.1016/j.jhazmat.2022.129762>, 2023b.
- Wang, K., Jia, R., Li, L., Jiang, R., and Qu, D.: Community structure of *Anaeromyxobacter* in Fe(III) reducing enriched cultures of paddy soils, *J. Soils Sed.*, 20, 1621-1631, <https://doi.org/10.1007/s11368-019-02529-7>, 2020b.

- Wang, Q., Song, X., Wei, C., Jin, P., Chen, X., Tang, Z., Li, K., Ding, X., and Fu, H.: In situ remediation of Cr(VI) contaminated groundwater by ZVI-PRB and the corresponding indigenous microbial community responses: a field-scale study, *Sci. Total Environ.*, 805, 150260, <https://doi.org/10.1016/j.scitotenv.2021.150260>, 2022.
- Yaashikaa, P. R., Kumar, P. S., Jeevanantham, S., and Saravanan, R.: A review on bioremediation approach for heavy metal detoxification and accumulation in plants, *Environ. Pollut.*, 301, 119035, <https://doi.org/10.1016/j.envpol.2022.119035>, 2022.
- Yang, Y., Wang, H., Zheng, Y., Zhu, B., Wu, X., and Zhao, F.: Extracellular electron transfer of *Methylophilus methylotrophs*, *Process Biochem.*, 94, 313-318, <https://doi.org/10.1016/j.procbio.2020.05.001>, 2020.
- Yin, Y., Chen, Y., and Wang, J.: Co-fermentation of sewage sludge and algae and Fe<sup>2+</sup> addition for enhancing hydrogen production, *International Journal of Hydrogen Energy*, 46, 8950-8960, <https://doi.org/10.1016/j.ijhydene.2021.01.009>, 2021.
- Zhang, J., Liu, Y., Sun, Y., Wang, H., Cao, X., and Li, X.: Effect of soil type on heavy metals removal in bioelectrochemical system, *Bioelectrochemistry*, 136, 107596, <https://doi.org/10.1016/j.bioelechem.2020.107596>, 2020.
- Zhang, Y., Zheng, S., Hao, Q., Wang, O., and Liu, F.: Respiratory electrogen *Geobacter* boosts hydrogen production efficiency of fermentative electrotroph *Clostridium pasteurianum*, *Chem. Eng. J.*, 456, 141069, <https://doi.org/10.1016/j.cej.2022.141069>, 2023.
- Zhang, Y., Shen, G., Hu, S., He, Y., Li, P., and Zhang, B.: Deciphering of antibiotic resistance genes (ARGs) and potential abiotic indicators for the emergence of ARGs in an interconnected lake-river-reservoir system, *J. Hazard. Mater.*, 410, 124552, <https://doi.org/10.1016/j.jhazmat.2020.124552>, 2021.
- Zhang, Y., Gu, A. Z., Cen, T., Li, X., He, M., Li, D., and Chen, J.: Sub-inhibitory concentrations of heavy metals facilitate the horizontal transfer of plasmid-mediated antibiotic resistance genes in water environment, *Environ. Pollut.*, 237, 74-82, <https://doi.org/10.1016/j.envpol.2018.01.032>, 2018.
- Zhu, J., Zhang, T., Zhu, N., Feng, C., Zhou, S., and Dahlgren, R. A.: Bioelectricity generation by wetland plant-sediment microbial fuel cells (P-SMFC) and effects on the transformation and mobility of arsenic and heavy metals in sediment, *Environ. Geochem. Health*, 41, 2157-2168, <https://doi.org/10.1007/s10653-019-00266-x>, 2019.